

Magnetic studies of Sn^{2+} – Sn^{4+} -substituted barium hexaferrites synthesized by mechanical alloying

A. González-Angeles^{a,*}, G. Mendoza-Suárez^a, A. Grusková^b,
R. Dosoudil^c, R. Ortega-Zempoalteca^d

^a *Cinvestav-Salttillo, Carr. Saltillo-Mty. km. 13, P.O. Box 663, 25000 Saltillo, Coahuila, Mexico*

^b *Department of Electrotechnology, Faculty of Electrical Engineering and Information Technology, (FEEIT) Slovak University of Technology, Ilkovičova 3, 812 19 Bratislava, Slovakia*

^c *Department of Electromagnetic Theory, (FEEIT-SUT), Slovakia*

^d *Instituto de Investigaciones en Materiales, Departamento de Cerámicos y Metálicos, UNAM, P. O. Box 73-360, Mexico D.F. 04510, Mexico*

Received 31 January 2004; received in revised form 10 May 2004; accepted 15 May 2004

Available online 21 June 2004

Abstract

The effect of Sn^{2+} – Sn^{4+} mixture on magnetic properties of BaM has been studied by Mössbauer spectroscopy and vibrating sample magnetometry. The results show that the magnetization reached a maximum for $x=0.2$ and then diminished. Mössbauer spectra showed that Sn^{2+} – Sn^{4+} ions preferentially occupy 2b and 4f₂ sites, followed by 4f₁ and 2a sites; whilst the 12k was the least affected by the substitution. The preference for the 4f₂ and 4f₁ sites is responsible for the increase in the magnetization at low substitutions, due to their spin down configuration. At $x \geq 0.3$ values, a steep drop of both M_s and M_r was recorded, which might be due to the appearance of small amounts of tin oxide (SnO_2) as a secondary phase. A large variation of the intrinsic coercivity, H_{ci} , (4.8 to 0.909 kOe) was obtained as a function of the substitution. The rapid decrease of H_{ci} has its origin in the preference of Sn^{2+} – Sn^{4+} ions for the 2b and 4f₂ sites.

© 2004 Elsevier B.V. All rights reserved.

PACS: 75.50; 74.25.Ha; 75.50.Ss; 33.45.+x; 71.20Ps

Keywords: Substitution effects; Magnetic properties; Mössbauer spectra; Hexagonal ferrites

1. Introduction

The hexagonal ferrites ($\text{BaFe}_{12}\text{O}_{19}$) have been widely studied as potential materials for perpendicular magnetic recording and microwave absorption. For these applications, high saturation magnetization, a suitable coercivity and low temperature coefficients of coercivity and remanence are desired. To obtain good quality of barium ferrite materials, various methods have been used for their preparation and a large number of investigations have been carried out to modify the magnetic parameters by replacing Fe^{3+} with different cationic combination [1]. In order to obtain hexagonal ferrites with improved characteristics for applications in the field of magnetic recording, a new chemical substitution was obtained (Sn^{2+} – Sn^{4+}), which showed to be

effective in reducing the magnetocrystalline anisotropy and enhancing M_s . For the understanding of the origin of these properties, it is necessary to elucidate which crystallographic sites the Sn^{2+} and Sn^{4+} ions prefer to occupy.

The ^{57}Fe Mössbauer effect is an ideal technique to investigate the site occupancy in compounds with multiple sublattices, such as BaM. In this paper, we present the results of a Mössbauer and magnetic study in samples of $\text{BaFe}_{12-2x}(\text{Sn}^{2+}\text{–}\text{Sn}^{4+})_x\text{O}_{19}$ with x ranging from 0 to 0.4.

2. Experiment

Polycrystalline samples of $\text{BaFe}_{12-2x}(\text{Sn}^{2+}\text{–}\text{Sn}^{4+})_x\text{O}_{19}$ ($\text{BaM}_{\text{Sn-Sn}}$) with $0 \leq x \leq 0.4$ were synthesized by attrition milling. BaCO_3 , Fe_2O_3 , SnO and SnO_2 were used as raw materials, all of 98% of purity. Milling was performed in a Segvay attritor using a ball/powder ratio of 15 and an Fe/Ba ratio of 10. The powders were milled for 28 h in air using an

* Corresponding author. Tel.: +52-8444389600, fax: +52-438-9610.

E-mail address: gangeles@salttillo.cinvestav.mx

(A. González-Angeles).

angular velocity of 400 rpm and 250 ml of benzene to avoid agglomeration at the mill bottom. After mechanical milling, the samples were annealed at 1050 °C for 1.5 h.

The identification of the crystalline phases in the samples was performed with an X-pert Phillips diffractometer using Cu-K α radiation. The magnetization curves of BaM $_{Sn-Sn}$ were measured in an applied external magnetic field of 12 kOe at room temperature, using a Lake Shore 7300 vibrating sample magnetometer. Mössbauer spectroscopy studies were performed with a spectrometer operated at a constant mode, using a $^{57}\text{Co/Rh}$ γ -ray source to determinate the distribution of Sn $^{2+}$ and Sn $^{4+}$ in the hexagonal structure. The Mössbauer spectra were fitted using the NORMOS software package. The temperature dependence of the magnetic susceptibility, $\chi(\theta)$ was determined by bridge method in an alternating magnetic field of 4.52 Oe at 1 kHz. The measurements were performed up to 730 °C at a constant heating rate of 4 °C/min. To obtain information on both the morphology and particle distribution, a Philips XL 30 scanning electron microscope (SEM) was used.

3. Results and discussions

The X-ray diffraction studies of the Sn $^{2+}$ -Sn $^{4+}$ substituted barium ferrites (Fig. 1), revealed that BaM was the only phase present for $x < 0.3$, at least, within the errors inherent to the technique. For $x > 0.2$, SnO $_2$ appeared as a secondary phase, whose formation occurred presumably to the expense of less stable Sn $^{2+}$ ion, owing to the milling conditions.

Mössbauer spectra at room temperature for BaM $_{Sn-Sn}$ are shown in Fig. 2. Hyperfine magnetic field, the quadrupole splitting, the isomer shift, the angle θ between the hyperfine field and the principal axis of the electric field gradient tensor, the line-width at half-maximum and the

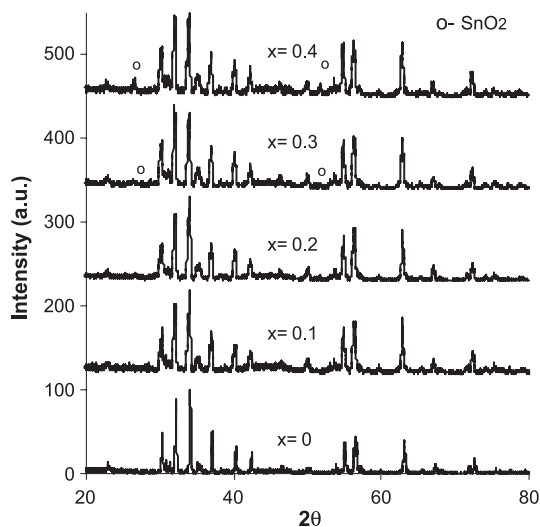


Fig. 1. X-ray diffraction patterns for BaM $_{Sn-Sn}$ showing only the magnetoplumbite structure up to $x = 0.2$.

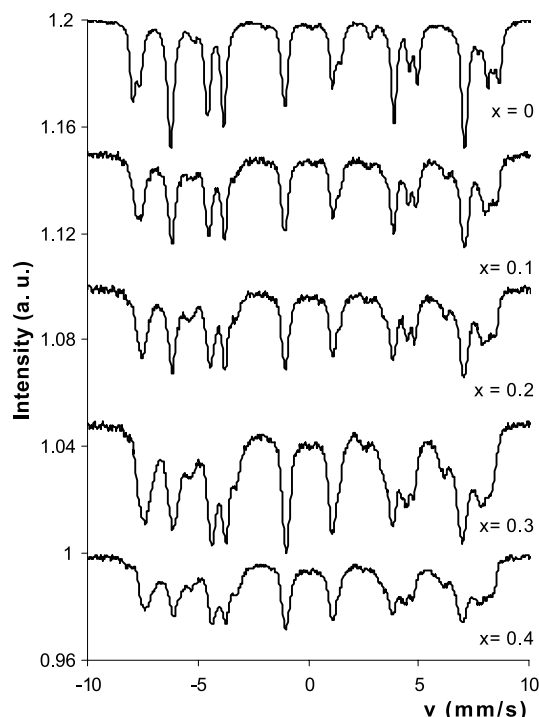


Fig. 2. ^{57}Fe Mössbauer spectra at room temperature for BaM $_{Sn-Sn}$ samples ($x = 0-0.4$). Note the change in the intensity and width as the substitution increases.

total intensity were the fitted parameters for each of the five Zeeman patterns. This gave a maximum number of adjustable parameters of 30, which correspond to the five different Fe $^{3+}$ sites (4f $_2$, 2a, 4f $_1$, 12k and 2b) in the magnetoplumbite structure [2,3]. The intensity and shape of the spectra changed as x increased, indicating that the substitution of iron ions by the diamagnetic ions took place. The spectra for $x > 0$ were fitted with four sextet subpatterns, corresponding to five different crystallographic sites, 4f $_2$, 2a + 4f $_1$, 12k and 2b, respectively. The hyperfine fields for 2a and 4f $_1$ sites are nearly equal, so that these two subpatterns could not be resolved. As x increased, 12k site was fitted with two

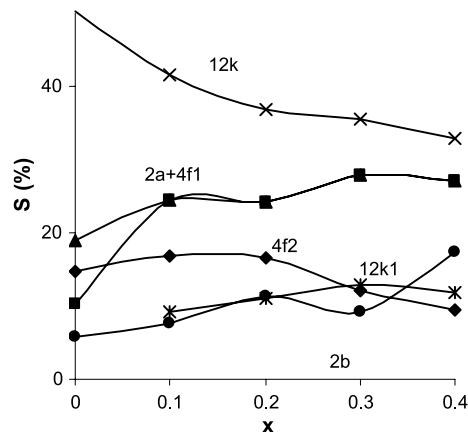


Fig. 3. Variation of the relative spectral areas S (%) with increasing substitution ratio.

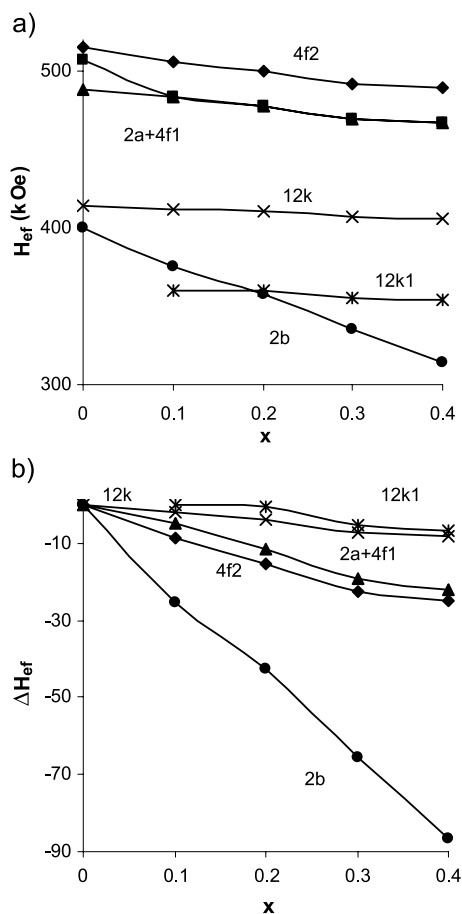


Fig. 4. Variation of (a) hyperfine fields (H_{ef} ; kOe) and (b) ΔH_{ef} (kOe) as a function of the substitution x .

subpatterns, 12k and 12k₁. This could be related to changes in the environment or neighbours of the iron ions at the 12k site when the substitutions take place in R block. On the other hand, the appearance of an additional subspectrum for $x \geq 0.3$ was observed. This compound must possess iron ions to be detected by Mössbauer spectroscopy. It cannot be a (super) paramagnetic phase because it would be mani-

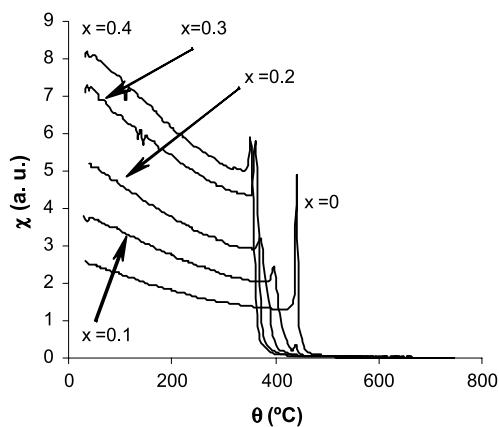


Fig. 5. Temperature dependence of the magnetic susceptibility of $\text{BaM}_{\text{Sn}-1-x}\text{Sn}_x$. Note the increase of χ with substitution.

Table 1
Variation of the magnetic properties with the substitution grade

x	M_s (emu/g)	H_{ci} (kOe)	M_r (emu/g)	T_c ($^{\circ}\text{C}$)
0.0	60.9	4.79	34.8	442
0.1	64.0	2.89	33.5	399
0.2	66.15	1.977	33.15	373
0.3	65.0	1.054	26.8	361
0.4	59.8	0.909	22.3	350

fested as a doublet spectrum. Therefore, it is believed to correspond to a nonmagnetic probably amorphous phase, in this case it is reasonable that it was not identified in the X-ray pattern.

The variation of the relative areas (S , %) and hyperfine fields (H_{ef}) with increasing doping rate is shown in Figs. 3 and 4, respectively. From Fig. 4b, it can be observed that ΔH_{ef} was maximum for the bipyramidal 2b site, followed by 4f₂ and 2a + 4f₁ sites, whilst the octahedral 12k site was the least affected by the substitution. According to previous reports [4,5] and taking into account the difference of ionic radii between Sn^{2+} (1.12 Å) and Sn^{4+} (0.71 Å) ions, it can be assumed that Sn^{2+} ions substitute in the octahedral (4f₂ and 2a) sites, whereas Sn^{4+} ions prefer the tetrahedral (4f₁) and bipyramidal (2b) sites. The latter assumption can be further supported by the fact that the octahedral interstitial site is larger than the tetrahedral site.

The temperature dependence of the magnetic susceptibility, χ (θ) was measured in a full automatic device, where the sample (0.2 cm³–1 g) was heated at a constant rate of 5 $^{\circ}\text{C}/\text{min}$ with a step between each individual measurement of 5 $^{\circ}\text{C}$ [6]. These measurements (Fig. 5) showed that χ increased with the Sn^{2+} – Sn^{4+} substitution. This can be explained taking into account that the magnetic susceptibility depends partly on the contribution of noncollinear spins in the magnetic structure. Consequently, it increases due to the disruption of the collinear uniaxial

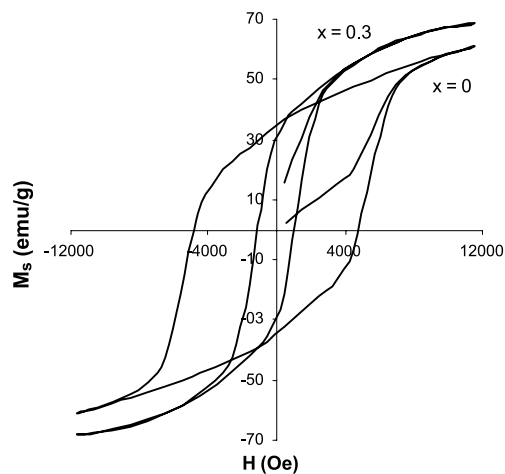


Fig. 6. Hysteresis loops for $\text{BaM}_{\text{Sn}-1-x}\text{Sn}_x$ compounds showing the increase of the susceptibility and the decrease of the coercivity as the substitution increases.

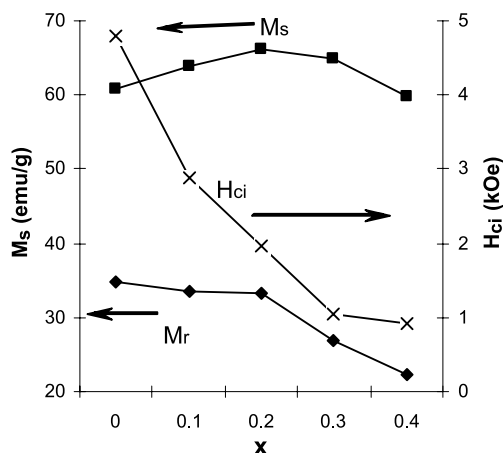


Fig. 7. Saturation (M_s) and remanent (M_r) magnetization and coercivity (H_{ci}) as a function of the substitution.

magnetic structure by the replacement of Fe^{3+} ions, by either nonmagnetic or less magnetic cations. Table 1 summarizes the Curie temperatures, T_c , determined from the Hopkinson's effect, shown in the $\chi(\theta)$ curves (Fig. 5). The increase of the substitution level caused a T_c decrease of $\sim 21\%$. This could be explained by the reduction in the strength of superexchange interactions among iron ions [7]. Although, the Hopkinson's effect could also be shifted to lower temperatures due to the presence of the secondary phase (SnO_2).

Fig. 6 shows the hysteresis loops for the samples with substitution values of $x=0$ and 0.3 obtained by vibrating sample magnetometry. The effect of the $Sn^{2+}-Sn^{4+}$ substitution on the hysteresis curve shape and the magnetic properties of the samples can be observed perfectly. From the slope corresponding to the primary magnetization

curves, qualitative information on the magnetic susceptibility change with the substitution can be obtained.

The variation of magnetic properties with the substitution level x is shown in both Table 1 and Fig. 7. It can be seen that M_s rise gradually up to a maximum at $x=0.2$ (increase $\sim 9\%$), decreasing beyond $x \geq 0.3$. The increase of M_s owes to the site preference occupancy of Sn^{4+} ($2b$ and $4f_1$) and Sn^{2+} ($4f_2$ and $2a$) ions. That means that Fe^{3+} ions with spin down ($4f_1$ and $4f_2$), which contributing negatively to total magnetization, are replaced, increasing the total M_s . On the other hand, the remanent magnetization, M_r , remained almost without change (diminution $\sim 5\%$) up to $x=0.2$, diminishing drastically (reduction $\sim 36\%$) only for compositions of $x \geq 0.3$, presumably due to the onset of the SnO_2 nucleation. The strong drop of H_{ci} (drop $\sim 81\%$) as x increased was related to reduction of the magnetocrystalline anisotropy, due to the replacement of iron ions at $2b$ bipyramidal sites, which have the greatest contribution to the anisotropy [7–9].

The morphology and the particle size distribution of BaM_{Sn-Sn} are shown in the micrographs of Fig. 8. All the particles showed nearly hexagonal platelet shape. The particle size in the micrograph seems to decrease as the substitution level increased up to $x=0.3$ and stayed well below $1 \mu m$. However, it is clear that other studies are necessary to find out the real crystalline size of the powders.

4. Conclusions

It was possible to synthesize $Sn^{2+}-Sn^{4+}$ substituted barium hexaferrites by mechanical alloying. These compounds possess the required microstructure and magnetic properties for high-density magnetic recording applica-

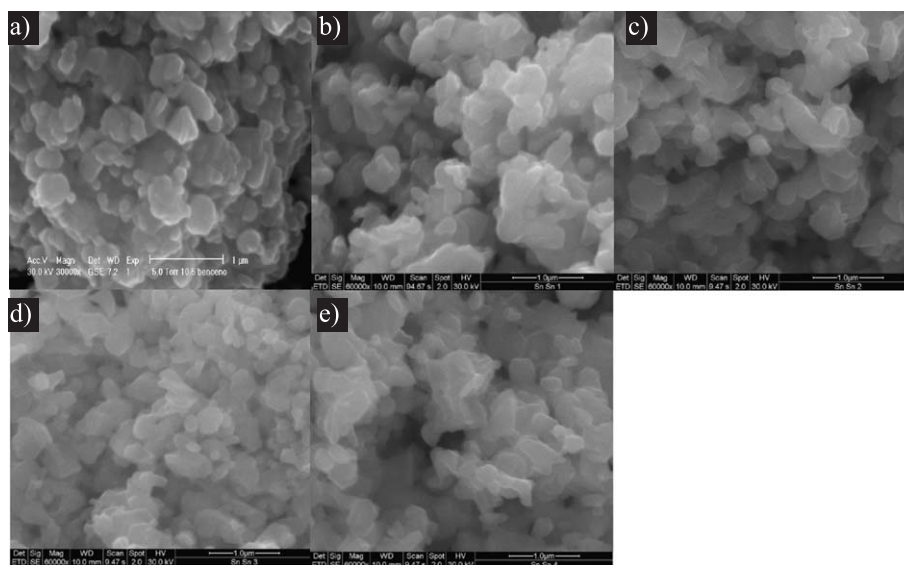


Fig. 8. SEM micrographs for BaM_{Sn-Sn} samples with (a) $x=0$, (b) $x=0.1$, (c) $x=0.2$, (d) $x=0.3$ and (e) $x=0.4$. The grain size is well below $1 \mu m$ and appears to decrease with substitution.

tions. The saturation magnetization increased moderately ($\sim 9\%$) for small levels of substitution. This enhancement is presumably related to the preferential occupation of Sn^{2+} and Sn^{4+} ions in $4f_2$ and $4f_1$ sites, respectively. By changing the substitution rate x , the coercivity could easily be controlled without a significant reduction of M_s . The steep reduction of M_r for $x \geq 0.3$ was likely due to the formation of SnO_2 . The strong reduction of H_{ci} ($\sim 81\%$) as x increased is related to reduction of the magnetocrystalline anisotropy, due to the substitution of Fe^{3+} ions firstly on the 2b bipyramidal and $4f_2$ octahedral sites. The magnetic susceptibility (χ) increased with the substitution x , which is believed to relate to the disappearance of some superexchange interactions among the iron ions. The rapid increase in the magnetic susceptibility as well as the large reduction in saturation magnetization at $x \geq 0.3$ could suggest that a noncollinear magnetic structure occurs due to spin canting. The Sn^{4+} cations substituted Fe^{3+} mainly on the bipyramidal (2b) and slightly on tetrahedral ($4f_1$) site, whilst the Sn^{2+} ions preferred the octahedral ($4f_2$ and 2a) sites. The reduction of T_c ($\sim 21\%$) demonstrates the gradual breakdown of magnetic ordering. Our results suggest that the Sn^{2+} – Sn^{4+} substitution can be a promising candidate for magnetic recording applications.

Acknowledgements

We would like to thank CONACyT-México for the support given to carry out this work under Project J28283U.

Special thanks also to Ing. Tóth and Jančárik, for the Mössbauer and magnetic susceptibility measurements, respectively. We are indebted to M. Papanová for her help in sample preparation. Our gratitude also goes to both Prof. J. Lipka and Ing. J. Santoyo-Salazar for their contributions to this work.

References

- [1] W. Wolski, *Jpn. J. Appl. Phys.* 9 (1990) 711–715.
- [2] J. Lipka, M. Miglierini, *J. Electr. Eng.* 45 (1994) 12–14.
- [3] J. Lipka, A. Grusková, M. Michalíková, M. Miglierini, J. Sláma, I. Thot, *J. Magn. Magn. Mater.* 140–144 (1995) 2209–2210.
- [4] A. González-Angeles, G. Mendoza-Suárez, A. Grusková, I. Tóth, V. Jančárik, M. Papanová, J.I. Escalante-García, *J. Magn. Magn. Mater.* 270 (2004) 77–83.
- [5] H.C. Fang, Z. Yang, C.K. Ong, Y. Li, C.S. Wang, *J. Magn. Magn. Mater.* 187 (1998) 129.
- [6] V. Jančárik, E. Ušák, *J. Electr. Eng.* 50 (1999) 63–138.
- [7] Z. Yang, C.S. Wang, X.H. Li, H.X. Zang, *Mater. Sci. Eng., B* 90 (2002) 142–145.
- [8] X. Batlle, X. Obradors, J. Rodríguez-Carbajal, M. Pernet, M.V. Cabanas, M. Vallet, *J. Appl. Phys.* 70 (1991) 1614.
- [9] J. Kreisel, H. Vincent, F. Tasset, P. Wolfers, *J. Magn. Magn. Mater.* 213 (2000) 262–270.